Kicked rotor and Anderson localization

Boulder School on Condensed Matter Physics, 2013

Dominique Delande
Laboratoire Kastler-Brossel, Université Pierre et Marie Curie, Ecole Normale Supérieure, CNRS; 4 Place Jussieu, F-75005 Paris, France

CONTENTS

INTRODUCTION: ANDERSON LOCALIZATION

I. LECTURE I: THE PERIODICALLY KICKED ROTOR

II. LECTURE II: EXPERIMENTS WITH THE PERIODICALLY KICKED ROTOR

III. LECTURE III: THE QUASI-PERIODICALLY KICKED ROTOR

A. The model

How can the kicked rotor be used to study Anderson localization in more than one dimension? The first idea is to use a higher-dimensional rotor with a classically chaotic dynamics and to kick it periodically. It turns out that this is not easily realized experimentally, as it requires to build a specially crafted spatial dependence[1]. Yet, remember that time and space have switched roles, and so a simpler idea is to use additional temporal dimensions rather than spatial dimensions. Instead of kicking the system periodically with kicks of constant strength, one may use a temporally quasi-periodic excitation. Various schemes have been used [2], but the one allowing to map on a multi-dimensional Anderson model uses a quasi-periodic modulation of the kick strength, the kicks being applied at fixed time interval [3].

We will be interested in a 3d Anderson model, obtained by adding two quasi-periods to the system:[27]

$$\mathcal{H}_{\rm qp} = \frac{p^2}{2} + \mathcal{K}(t)\cos x \sum_n \delta(t-n)\ , \tag{1}$$

with

$$\mathcal{K}(t) = K\left[1+\varepsilon\cos\left(\omega_2 t+\varphi_2\right)\cos\left(\omega_3 t+\varphi_3\right)\right]\ . \tag{2}$$

It is easy to write the classical evolution from kick n to kick $n+1$, exactly as we did for the periodically kicked rotor. One obtains:

$$\begin{cases} p_{n+1} = p_n + \mathcal{K}(n) \sin x_n \\ x_{n+1} = x_n + p_{n+1} \end{cases} \tag{3}$$

that is the same result than for the periodically kicked rotor, except that $\mathcal{K}$ now depends quasi-periodically on time.

Now where is the three dimensional aspect in this problem? The answer lies in a mapping of this quasi-periodic kicked rotor on a 3d kicked "pseudo"-rotor with the special initial condition of a "plane source", as follows.

B. The periodically kicked pseudo-rotor

Let us consider a 3d periodically kicked pseudo-rotor, whose Hamiltonian is:

$$\mathcal{H} = \frac{p_1^2}{2} + \omega_2 p_2 + \omega_3 p_3 + K \cos x_1 \left[1 + \varepsilon \cos x_2 \cos x_3\right] \sum_n \delta(t-n), \tag{4}$$

This is not a true rotor, because of the unusual form of the kinetic energy in directions 2 and 3, where it is a linear – instead of quadratic – function of the momentum, hence the name pseudo-rotor. Being a periodic system, we can again write the map over one period:

$$\begin{aligned} p_{1_{n+1}} &= p_{1_n} + K \sin x_{1_n} (1 + \varepsilon \cos x_{2_n} \cos x_{3_n}) \ , \\ p_{2_{n+1}} &= p_{2_n} + K\varepsilon \cos x_{1_n} \sin x_{2_n} \cos x_{3_n} \ , \\ p_{3_{n+1}} &= p_{3_n} + K\varepsilon \cos x_{1_n} \cos x_{2_n} \sin x_{3_n} \ , \\ x_{1_{n+1}} &= x_{1_n} + p_{1_{n+1}} \ , \\ x_{2_{n+1}} &= x_{2_n} + \omega_2 \ , \\ x_{3_{n+1}} &= x_{1_n} + \omega_3 \ . \end{aligned} \tag{5}$$

The last two equations are trivially integrated: $x_{2_n} = x_{2_0} + n\omega_2$ and similarly for x_3. If we now start with the initial condition $x_{2_0} = \varphi_2, x_{3_0} = \varphi_3$, it is straightforward to realized that the mapping for p_1 and n_1 is *exactly* the same than the mapping (3) of the quasi-periodically kicked rotor. In other words, the classical dynamics of the kicked pseudo-rotor along the direction 1 is strictly identical to the one of the quasi-periodically kicked rotor.

The same mapping exists for the quantum evolution. Consider the evolution of a wavefunction Ψ with the initial condition

$$\Psi(x_1, x_2, x_3, t=0) \equiv \psi(x_1, t=0)\delta(x_2 - \varphi_2)\delta(x_3 - \varphi_3). \tag{6}$$

This initial state, perfectly localized in x_2 and x_3 and therefore entirely delocalized in the conjugate momenta p_2 and p_3, is a "plane source" in momentum space [4]. A simple calculation shows that the stroboscopic evolution of Ψ under (4) coincides exactly with the evolution of the initial state $\psi(x = x_1, t = 0)$ under the Hamiltonian (1) of the quasi-periodically kicked rotor (for details, see [5]). An experiment with the quasi-periodic kicked rotor can thus be seen as a localization experiment in a 3d disordered system, where localization is actually observed in the direction perpendicular to the plane source. In other words, the situation is comparable to a transmission experiment where the sample is illuminated by a plane wave and the exponential localization is only measured along the wave vector direction. Therefore, the behavior of the quasi-periodic kicked rotor (1) matches *all* dynamic properties of the quantum 3d kicked pseudo-rotor.

For sufficiently large K and not too small ε, the classical dynamics of the pseudo-rotor is a chaotic diffusion in momentum space. Indeed, coupling to the strongly chaotic direction 1 is sufficient to make the dyanamics along directions 2 and 3 also diffusive [6]. However, the diffusion tensor is not isotropic. It can be computed like for the periodically kicked rotor, that is assuming no position-momentum correlation and complete delocalization in configuration space. One obtains for the anisotropic diffusion tensor (for ε smaller than unity):

$$D_{11} \approx (K^2/4)(1 + \varepsilon^2/4) \ , \tag{7}$$

$$D_{22} \approx K^2\varepsilon^2/16 \ , \tag{8}$$

$$D_{33} \approx K^2\varepsilon^2/16 \ , \tag{9}$$

$$D_{i\neq j} \approx 0 \ . \tag{10}$$

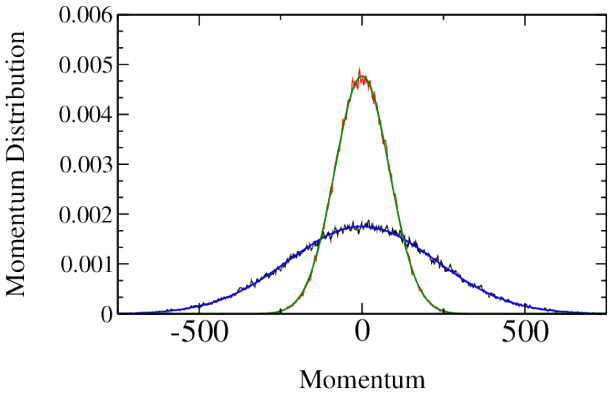

FIG. 1. Final momentum distributions along p_1 (in black) and p_2 (in red), the distribution along p_3 being approximately identical to that along p_2. After 1000 kicks, they display all a Gaussian shape characteristic of a diffusive motion. The blue and green curves are fits by a Gaussian which do not show any statistically significant deviation. Parameters are $K = 10$, $\varepsilon = 0.8$, $\omega_2 = 2\pi\sqrt{5}$ and $\omega_3 = 2\pi\sqrt{13}$.

The coupling between the 3 degrees of freedom tend to reduce the stability of phase space structures at low K. For example, accelerator modes – which exist in the periodically kicked rotor – disappear for rather small values of ε. Altogether, for $\varepsilon > 0.1$, the classical dynamics can be considered as an anisotropic chaotic diffusion down to $K = 3-4$.

Note: the script `qpkr_final_momentum_distribution.py` generates the distribution of final momentum along the three directions 1, 2 and 3 (only direction 1 is the physical dimension) starting from a ensemble of trajectories initially located near p=0. For sufficiently large K (of the order of 3), it is a Gaussian, showing that the classical dynamics of the QPKR is a deterministic chaotic diffusion. Interestingly, less deviations from pure Gaussian are observed for the QPKR than for the KR (see corresponding script `standard_map_final_momentum_distribution.py`). The script `qpkr_p2_vs_time.py` shows the linear increase of p^2 with time.

C. Anderson transition

As for the standard 3d kicked rotor (4), the quantum dynamics of the periodically kicked pseudo-rotor can be studied using the Floquet states via mapping to a 3d Anderson-like model:

$$\epsilon_{\mathbf{m}}\Phi_{\mathbf{m}} + \sum_{\mathbf{r}\neq 0} W_{\mathbf{r}}\Phi_{\mathbf{m}-\mathbf{r}} = -W_{\mathbf{0}}\Phi_{\mathbf{m}} \ , \tag{11}$$

where $\mathbf{m} \equiv (m_1, m_2, m_3)$ labels sites in a 3d cubic lattice, the on-site energy $\epsilon_{\mathbf{m}}$ is

$$\epsilon_{\mathbf{m}} = \tan\left\{\frac{1}{2}\left[\omega - \left(\hbar\frac{{m_1}^2}{2} + \omega_2 m_2 + \omega_3 m_3\right)\right]\right\} \ , \tag{12}$$

and the hopping amplitudes $W_{\mathbf{r}}$ are the Fourier expansion coefficients of

$$W(x_1, x_2, x_3) = \tan\left[K\cos x_1(1 + \varepsilon\cos x_2\cos x_3)/\,2\hbar\right] . \tag{13}$$

A necessary condition for localization is obviously that $\epsilon_{\mathbf{m}}$ not be periodic. This is achieved if $(\hbar, \omega_2, \omega_3, \pi)$ are incommensurate. When these conditions are verified, localization effects as predicted for the 3d Anderson model are expected, namely either a diffusive or a localized regime. Localized states would be observed if the disorder strength is large compared to the hopping. In the case of the model (11), the amplitude of the disorder is fixed, but the hopping amplitudes can be controlled by changing the stochasticity parameter K (and/or the modulation amplitude ε): $W_{\mathbf{r}}$ is easily seen to increase with K. In other words, the larger K, the smaller the disorder. One thus expects to observe diffusion for large stochasticity K and/or modulation amplitude ε (small disorder) and localization for small K and/or ε (large disorder). It should be emphasized that *stricto sensu* there is no mobility edge in our system that would separate localized from delocalized eigenstates. Depending on the parameters $K, \hbar, \varepsilon, \omega_2, \omega_3$, either *all* Floquet states are localized or all are delocalized. The boundary of the metal-insulator transition is in the $(K, \hbar, \varepsilon, \omega_2, \omega_3)$-parameter space. As seen below, K and ε are the primarily important parameters.

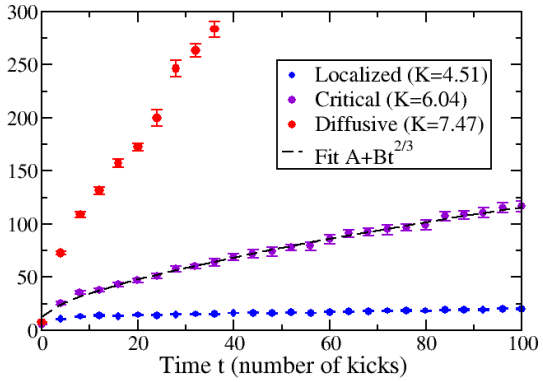

FIG. 2. Experimentally measured temporal dynamics of the quasi-periodically kicked rotor, for increasing values of the kick strength. The average kinetic energy $\langle p^2(t)\rangle$ tends to a constant in the localized regime (lower blue curve) increases linearly with time in the diffusive regime (upper red curve). At the critical point $K = K_c \approx 6.04$ (middle purple curve), anomalous diffusion $\langle p^2(t)\rangle \sim t^{2/3}$ (dashed curve) is clearly observed.

In the experiment performed at the University of Lille [7], kicks are applied to atoms with an initially narrow momentum distribution, and the final momentum distribution is measured using velocity-selective Raman transitions [28]. Figure 2 shows the experimental data. For large disorder, one clearly sees the initial diffusive phase and the freezing of the quantum dynamics in the localized regime (lower curve). In the diffusive regime (upper curve), $\langle p^2(t)\rangle$ is seen to increase linearly with time. The intermediate curve displays an anomalous diffusion $\langle p^2(t)\rangle \sim t^{2/3}$.

Why is this exponent 2/3? It is in fact a prediction of the scaling theory. In its standard form, the theory focuses on the scaling of the conductance g with the size L of the system:

$$g(L) = \sigma(L) L^{d-2} \tag{14}$$

where $\sigma(L)$ is the conductivity of the medium, proportional to the size-dependent diffusion constant $D(L)$. How to pass from the size L to the time t which is the scaling variable for the kicked rotor? It $t(L)$ is the characteristic time associated with size L (in other words, the time needed for the system at the critical point to diffuse over a size L), one has $D(L)t(L) \propto L^2$. At the critical point, $g(L)$ is independent of L; thus, from eq. (14), one has $D(L) \propto L^{2-d}$. By combining these two equations, we have $t(L) \propto L^d$ or $L \propto t^{1/d}$. Thus, the average value of $\langle p^2(t)\rangle$ increases like $D(L)t(L) \propto L^2 \propto t^{2/d}$, hence the 2/3 anomalous exponent in 3d. Only exactly at the unstable critical point will the anomalous diffusion subsist for arbitrarily long times. At slightly larger (resp. smaller) K, the motion will eventually turn diffusive (resp. localized) at long time. Experimental constraints prevent the observation beyond 150-200 kicks. Numerical simulations may extend much beyond: it has been checked that the anomalous diffusion with exponent 2/3 is followed for at least 10^8 kicks [5].

Since in numerical or experimental practice one always works in finite-size systems, we should emphasize that there is an important difference between a true metal-insulator transition and a cross-over between two limiting behaviors. For example, consider the simplest 1d situation where the dynamics eventually localizes for sure, with a localization time depending on the kick strength K. Over a finite experimental time, one may observe an apparently diffusive behavior if the localization time is longer than the duration of the experiment [29]. An intermediate situation with the localization time comparable to the duration of the experiment could produce data looking like anomalous diffusion. However, this could be only a transient behavior and a longer measurement will eventually show localization. In contrast, the $t^{2/3}$ behavior at the critical point of the Anderson transition is not a transient behavior, it extends to infinity, highlighting the scale-free behavior with fluctuations of all sizes present right at the critical point. Thus, the quantity playing the role of the conductance for the kicked rotor is nothing but:

$$\Lambda(t) = \frac{\langle p^2(t)\rangle}{t^{2/3}} \tag{15}$$

It is independent of time (for sufficiently long time, in order to avoid finite-size effects) at the critical point of the Anderson transition.

Note: The script `qpkr_quantum_dynamics.py` computes the temporal quantum evolution of the QPKR over many kicks. It outputs both $\langle p^2\rangle$ and the probability density in momentum space $\langle|\psi(p)|^2\rangle$ at the final time. This is the most important script for "observing" the Anderson transition. With the present set of parameters, it performs 3 successive

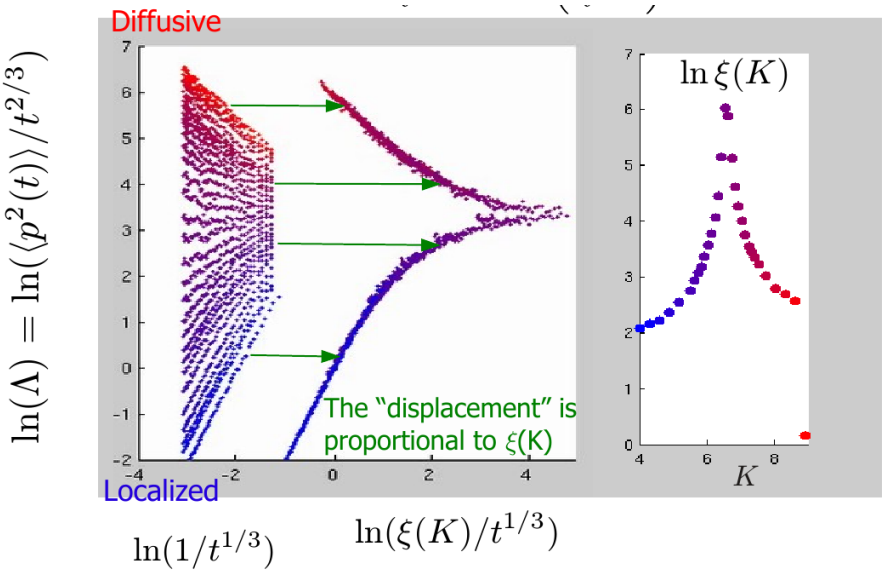

FIG. 3. Principle of the finite-time-scaling procedure. The raw data displaying $\Lambda(t)$ vs. $t^{-1/3}$ at various K values (left) are displaced horizontally so that to collapse as well as possible on a single scaling function, with an upper diffusive branch and a lower localized branch (middle). The displacement $\xi(K)$ is shown on the left part and has a singularity at the critical point K_c. The position of the tip of the scaling function gives the critical "conductance" Λ_c.

runs in the localized, critical and diffusive regimes. The data in `qpkr_p2_vs_time_quantum.dat` should be plotted in log-log scale to observe the anomalous diffusion at the critical point. Similarly, the momentum distributions in `qpkr_quantum_momentum_distribution.dat` display a localized exponential, a Airy function and a diffusive Gaussian.

D. Finite-time scaling

The unavoidable experimental limitation by finite size can also be turned into a powerful tool of analysis. It is known as finite-size scaling [8] and has its roots in the scaling properties observed in the vicinity of the transition. The idea is that all results, obtained for various values of parameters and time, are described by a universal scaling law depending on a single parameter, viz. the distance to the critical manifold. Close to the transition, there is only one characteristic length (which diverges at the critical point) and all details below this scale are irrelevant. Such an approach has been extremely successful to extract critical parameters from numerical simulations of the Anderson model for various system sizes. The approach has been transposed to the kicked rotor—see [5, 9] for details—and makes it possible to extract the localization length (in momentum space) from numerical or experimental data acquired over a restricted time interval. The one-parameter scaling hypothesis states that all data can be reduced to a universal scaling function F (actually, this "function" has two branches, a localized one and a diffusive one), and a localization length depending on the external parameters, in our case K, ε and $\hbar$ [30]:

$$\Lambda(t) = \frac{\langle p^2(t)\rangle}{t^{2/3}} = F\left(\frac{\xi(K,\varepsilon,\hbar)}{t^{1/3}}\right) \tag{16}$$

Although there are 3 relevant parameters which could be varies $(K, \varepsilon, \hbar)$, for practical reasons, $\hbar$ (that is the kicking period) is kept fixed during an experimental run, while either K, ε or both at the same time are varied. To observe a transition as well defined as possible, it is advisable to cross the critical line, see section III F as fast as possible, that is "at right angle", thus by simultaneously increasing K and ϵ. Then, by gathering experimental (or numerical) results got at increasing times and various K values, one can, by collapsing them on a single scaling function F, extract both F and the localization length $\xi(K)$. The procedure is shown in fig. 3.

The results extracted from the experimental data are shown in fig. 4. As expected, the charateristic length $\xi(K)$ (the localization length on the insulator side) has a pronounced maximum around $K =$, indicating that this is the position of the critical point. The divergence is smoothed by experimental imperfections and the finite duration of experiments. It is nevertheless possible to extract the critical exponent of the transition, by a simple fit in the vicinity

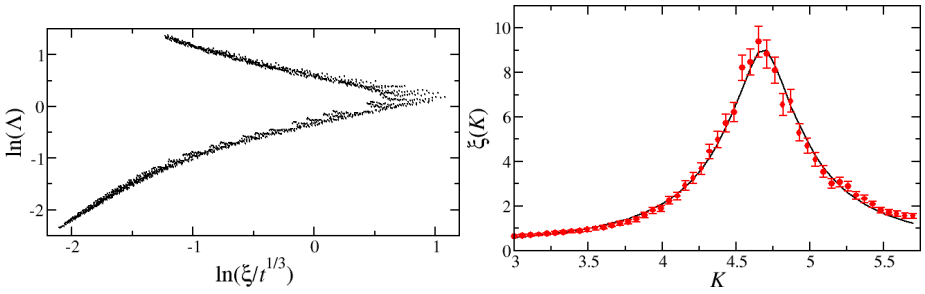

FIG. 4. Scaling function F, eq. (16 (left), and characteristic length $\xi(K)$ (for localization in momentum space)(right) extracted from real experiments on the quasi-periodically kicked rotor, in the vicinity of the metal-insulator Anderson transition [11]. Finite-size scaling is used. The characteristic length is proportional to the localization length on the insulating side, and to the inverse of the diffusion constant on the metallic side. It has an algebraic divergence $1/|K - K_c|^\nu$ at the transition, smoothed by finite size and decoherence. It is however possible to extract a rather precise estimate of the critical exponent ν.

of the transition:

$$1/\xi(K) = \alpha|K - K_c|^\nu + \beta \tag{17}$$

where β is a parameter taking into account the unavoidable cut-offs.

For the numerical experiments, one finds $\nu = 1.58 \pm 0.01$ in perfect agreement with the best determination on the Anderson model. Moreover, it has been checked that this exponent is universal, i.e. independent of the microscopic details such as the choice of the parameters $\hbar, \omega_2, \omega_3$ [10]. This is an additional confirmation that the transition observed is actually the metal-insulator Anderson transition.

E. Universality

A key property of the Anderson transition is that the critical exponent ν does not depend on any microscopic details such as the value of a parameter (the position of the critical point, on the other hand, depends on such details). We have therefore varied the parameters $\omega_2, \omega_3, \hbar$ as well as the path followed in the (K, ε) plane to cross the critical line and measured systematically the critical exponent. The raw results are shown in Table I and the critical exponent (with its error bars) shown in fig. 5. The 9 sets of data are compatible with the value $\nu = 1.58$ obtained from the numerical experiments [10], which is also the value obtained on the standard Anderson model [12]. The value extracted from these experimental results is $\nu = 1.63 \pm 0.05$. It definitely excludes the value $\nu = 1$ observed in solid-state experiments [13]. Most probably, electron-electron interactions are responsible for the breakdown of the Anderson scenario in real solid-state samples. Cold atoms as used in the kicked rotor experiments do not suffer from this drawback and allowed for the first unbiased measurement of the critical exponent.

Two additional remarks can be made. Firstly, the critical point is the same for sets A and B which differ only by the values of ω_2 and ω_3. This is expected, as their only effect is to modify which realizations of the disorder are taken, which should not affect the average values. Secondly, note that sets H and I have the same parameters, the only difference being how the δ-peaks are produced: they use different laser intensitiy/duration producing the same K. This produces a small change in both K_c and ν, showing that imperfections are always present in real experiments.

F. Self-consistent theory of localization

We have not yet computed, even approximately, the boundary between diffusive and localized motion, that is the critical line in the (K, ϵ) plane.

For this task, we will use the self-consistent theory of localization [14, 15]. The starting point is the so-called weak localization correction to the diffusion constant, due to constructive interference between paths which follow the same closed loop, but in opposite direction [16]. For the perodic or quasi-periodic kicked rotor in dimension d, it gives a frequency-dependent diffusion tensor [17]:

$$\mathcal{D}_{ii}(\omega) = D_{ii} - 2\hbar D_{ii} \int \frac{d^d \boldsymbol{q}}{(2\pi)^d} \frac{1}{-i\omega + \sum_j D_{jj} q_j^2} \ . \tag{18}$$

	$\hbar$	$\frac{\omega_2}{2\pi}$	$\frac{\omega_3}{2\pi}$	Path in (K,ε)	K_c	ν
A	2.89	$\sqrt{5}$	$\sqrt{13}$	4,0.1 → 8,0.8	6.67	1.63±0.06
B	2.89	$\sqrt{7}$	$\sqrt{17}$	4,0.1 → 8,0.8	6.68	1.57±0.08
C	2.89	$\sqrt{5}$	$\sqrt{13}$	3,0.435 → 10,0.435	5.91	1.55±0.25
D	2.89	$\sqrt{5}$	$\sqrt{13}$	7.5,0 → 7.5,0.73	ε_c=0.448	1.67±0.18
E	2.00	$\sqrt{5}$	$\sqrt{13}$	3,0.1 → 5.7,0.73	4.69	1.64±0.08
F	2.31	$\sqrt{5}$	$\sqrt{13}$	4,0.1 → 9,0.8	6.07	1.68±0.06
G	2.47	$\sqrt{5}$	$\sqrt{13}$	4,0.1 → 9,0.8	5.61	1.55±0.10
H	3.46	$\sqrt{5}$	$\sqrt{13}$	4,0.1 → 9,0.8	6.86	1.66±0.12
I	3.46	$\sqrt{5}$	$\sqrt{13}$	4,0.1 → 9,0.8	7.06	1.70±0.12

TABLE I. The 9 sets of parameters used: $\hbar$, ω_2 and ω_3 control the microscopic details of the disorder, K controls the amplitude and ϵ the anisotropy of the hopping amplitudes. The critical point K_c depends on the various parameters but the critical exponent is universal. The weighted mean of the critical exponent is $\nu = 1.63 \pm 0.05$. The duration of the kicks is $\tau = 0.8\,\mu$s for sets A-H, and $\tau = 0.96\,\mu$s for set I.

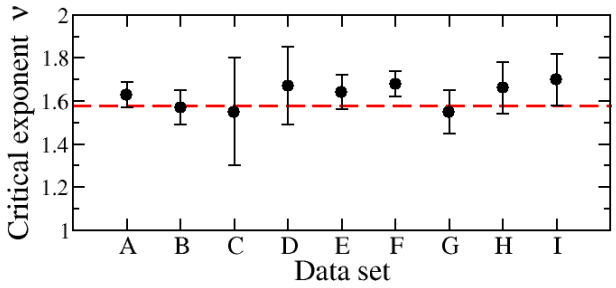

FIG. 5. Experimental test of the universality of the metal-insulator transition. The critical exponent ν, measured for 9 different sets of parameters A-I (see Tab. I), is *universal*, i.e. independent of the microscopic details. The error bars indicate one standard deviation, measured using the experimental uncertainties and a bootstrap technique. The dashed line is the commonly accepted value $\nu = 1.58$.

The self-consistent theory (which is actually not a real theory, but more a cooking recipe on how to include approximately higher order corrections) proposes to extend this equation to the strong disorder limit, where the correction is no longer small, by replacing self-consistently the raw diffusion constant in the correction term by the frequency-dependent one:

$$\mathcal{D}_{ii}(\omega) = D_{ii} - 2\hbar\mathcal{D}_{\rangle\rangle}(\omega) \int \frac{d^d\boldsymbol{q}}{(2\pi)^d} \frac{1}{-i\omega + \sum_j \mathcal{D}_{jj}(\omega) q_j^2} \,. \tag{19}$$

This leads to rather simple calculations, but sometimes surprisingly accurate results. For example, in 1d, for the periodically kicked rotor, it correctly predicts that all states are localized, and even gives the correct localization length $D/\hbar$ (see lecture I).

For the 3d quasi-periodically kicked rotor, the solution is a bit more complicated, because of a large q divergence of the integral, which must be regularized by e.g. cutting at the inverse of the mean-free path. If one chooses to a direction-dependent cutoff having the same anisotropy than the diffusion tensor, the equations can be solved exactly [18]. It predicts both the critical point and the critical conductance:

$$K_c(\varepsilon) = \left(\frac{2^3}{\pi^2}\right)^{1/3} \frac{\hbar}{(\varepsilon^2\sqrt{1+\varepsilon^2/4})^{1/3}} \tag{20}$$

$$\Lambda_c(\varepsilon) = \frac{3\hbar^2}{\Gamma(2/3)} \left(\frac{2}{\pi}\right)^{2/3} \left(\frac{1+\varepsilon^2/4}{\varepsilon^2}\right)^{2/3} \tag{21}$$

As shown in [18], these predictions are in good agreement with both numerical and experimental results.

Finally, the self-consistent theory also gives specific predictions for the behaviour of the system at the critical point. Not surprisingly, it there predicts that the diffusion tensor $\mathcal{D}(\omega)$ scales (in dimension 3) like $(-i\omega)^{1/3}$. This is nothing but the scaling law $\langle p^2(t)\rangle \propto t^{2/3}$. It also predicts the shape of the momentum distribution at long time (starting from

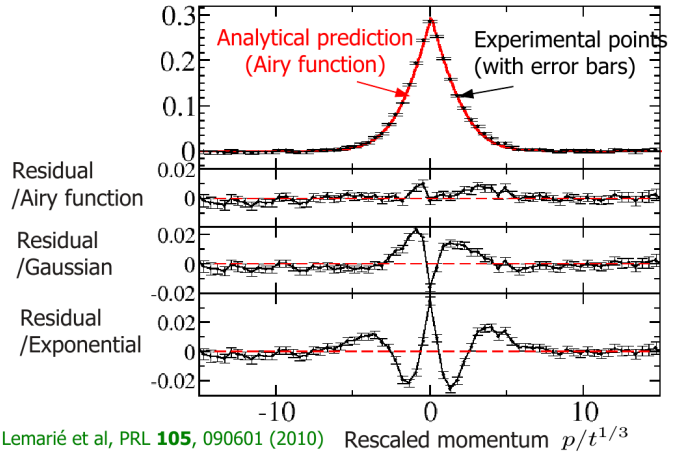

FIG. 6. Experimental data for the rescaled critical momentul density averaged over time (black circles with error bars) and a fit given by Eq. (22). The agreement is clearly excellent. The residual does not significantly differ from zero. Fits by an exponentially localized or a Gaussian distribution show significant deviations.

a localized initial distribution), that is the intensity average Green function in momentum space. The result is:

$$|\psi(p,t)|^2 \approx \frac{3}{2}\frac{\alpha}{\sqrt{\Lambda_c(\varepsilon)t^{2/3}}}\mathrm{Ai}\left[\alpha\sqrt{\frac{|p|^2}{\Lambda_c(\varepsilon)t^{2/3}}}\right] \tag{22}$$

where $\alpha = 3^{1/6}\Gamma(2/3)^{-1/2}$ and Ai the usual Airy function. This prediction has been tested experimentally [6], as shown in fig. 6. The agreement is excellent, with no statistically significant deviation.

This however does not mean that the self-consistent theory can predict only correct results. For example, it predicts $\nu = 1$ in dimension 3, a badly wrong prediction

G. Perspectives

Since the atom-atom contact interaction in a cold dilute gas is much smaller than the electron-electron Coulomb interaction in a solid sample, and since atoms are less easily lost than photons, cold atoms appear particularly suitable for precise measurements of the Anderson transition. Moreover, the possibility to picture wave functions directly opens the way to studies of fluctuations in the vicinity of the critical point [6], and may even permit to observe multifractal behavior [19] with matter waves. The flexibility of the kicked rotor could also be used to study the Anderson transition in lower dimensions (by reducing the number of quasi-periods) or, why not, even higher dimensions (by increasing it beyond 3).

Other possibilities could be to go to a different universality class. The unitary symmetry classe should be quite easily reached by breaking any anti-unitary symmetry such as the product of time-reversal and parity. Going to other symmetry classes would probably be more difficult. It would require an internal degree of freedom of the atoms (such as Zeeman hyperfine levels) with a coupling to the kicks depending on the internal state. There are for example ideas of observing the analog of the Quantum Hall Effect [22].

The incommensurate or commensurate character of the various parameters: $\hbar, \omega_i, \pi$ could also be used to study different regimes of quantum transport [23], or spectra with fractal properties, like the Hofstadter butterfly [24].

Very recently, the atomic kicked rotor periodically kicked with two standing waves with different periods has been studied experimentally in the group of D. Schneble in Stony Brook. It seems that the two incommensurate periods break any Anderson localization, restoring classical diffusion [25]. Similar results were obtained in Lille years ago, using two temporally incommensurate series of kicks [26].

Altogether, the main advantage of kicked rotor systems is that the tunable temporal sequence of kicks makes it possible to separate the notion of physical dimension (the system remains 1d) from the notion of "dynamical" dimension (which is 3 for the quasi-periodically kicked rotor). This may be very interesting when atom-atom interaction must be taken into account, e.g. in ultra-cold atomic Bose-Einstein condensates (or Fermi degenerate gases), as one can dream of using well established techniques such as bosonization and DMRG (see lectures of T. Giamarchi in this School) together with a complex temporal dynamics. Future will tell...

In any case, the kicked rotor is an attractive alternative to experiments on spatially disordered systems.

---

[1] J. Wang and A.M. Garcia-Garcia, "The Anderson transition in a 3d kicked rotor", Phys. Rev. E **79**, 036206 (2009).
[2] H. Lignier, J. Chabé, D. Delande, J.C. Garreau and P. Szriftgiser, "Reversible destruction of dynamical localization", Phys. Rev. Lett. **95**, 234101 (2005).
[3] G. Casati, I. Guarneri and D.L. Shepelyansky, "Anderson transition in a one-dimensional system with three incommensurable frequencies", Phys. Rev. Lett. **62**, 345–348 (1989).
[4] O.I. Lobkis and R.L. Weaver, "Self-consistent transport dynamics for localized waves", Phys. Rev. E **71**, 011112 (2005).
[5] G. Lemarié, J. Chabé, P. Szriftgiser, J.C. Garreau, B. Grémaud and D. Delande, "Observation of the Anderson Metal-Insulator Transition with Atomic Matter Waves: Theory and Experiment", Phys. Rev. A **80**, 043626 (2009).
[6] G. Lemarié, H. Lignier, D. Delande, P. Szriftgiser and J.C. Garreau, "Critical regime of the Anderson metal-insulator transition", Phys. Rev. Lett. **105**, 090601 (2010), arXiv:1005.1540.
[7] J. Chabé, G. Lemarié, B. Grémaud, D. Delande, P. Szriftgiser and J.C. Garreau, "Experimental observation of the Anderson metal-insulator transition with atomic matter waves" Phys. Rev. Lett. **101**, 255702 (2008).
[8] M.E. Fisher and M.N. Barber, "Scaling Theory for Finite-Size Effects in the Critical Region", Phys. Rev. Lett. **28**, 1516 (1972).
[9] G. Lemarié, "Transition d'Anderson avec des ondes de matière atomiques", PhD thesis, Université Pierre et Marie Curie, Paris (2009), http://tel.archives-ouvertes.fr/tel-00424399/fr/
[10] G. Lemarié, B. Grémaud and D. Delande, "Universality of the Anderson transition with the quasiperiodic kicked rotor", Europhys. Lett. **87**, 37007 (2009).
[11] M. Lopez, J.F. Clément, P. Szriftgiser, J.C. Garreau and D. Delande, Phys. Rev. Lett. **108**, 095701 (2012), arXiv:1108.0630: "Experimental Test of Universality of the Anderson Transition"
[12] K. Slevin and T. Ohtsuki, "Corrections to Scaling at the Anderson Transition", Phys. Rev. Lett. **82**, 382 (1999).
[13] S. Katsumoto, F. Komori, N. Sano and S. Kobayashi, "Fine tuning of metal-insulator transition in $Al_{0.3}Ga_{0.7}As$ using persistent photoconductivity", J. Phys. Soc. Jap. **56**, 2259 (1987).
[14] P. Woelfle and D. Vollhardt, arXiv:1004.3238.
[15] D. Vollhardt and P. Wölfle, "Self-consistent theory of Anderson localization", in: W. Hanke and Y. V. Kopaev, editors, *Electronic phase transitions* (Elsevier, Amsterdam, 1992)
[16] see the contribution of A. Andreev in this Summer School.
[17] A. Atland, Phys. Rev. Lett. **71**, 69 (1993).
[18] M. Lopez, J.-F. Clément, G. Lemarié, D. Delande, P. Szriftgiser and J. C. Garreau, New J. Phys. **15**, 065013 (2013), arXiv:1301.1615: "Phase diagram of the Anderson transition with atomic matter waves"
[19] S. Faez, A. Strybulevych, J.H. Page, A. Lagendijk and B.A. van Tiggelen, "Observation of multifractality at the Anderson localization transition of ultrasound in open three-dimensional media", Phys. Rev. Lett. **103**, 155703 (2009).
[20] J. Billy, V. Josse, Z. Zuo, A. Bernard, B. Hambrecht, P. Lugan, D. Clément, L. Sanchez-Palencia, Ph. Bouyer and A. Aspect, "Direct observation of Anderson localization of matter waves in a controlled disorder", Nature **453**, 891-894 (12 June 2008); Ph. Bouyer *et al.*, "Anderson localization of matter waves", Proceedings of the XXI ICAP Conference, R. Coté, Ph. L. Gould, M. Rozman and W. W. Smith eds., World Scientific (2008).
[21] P. Lugan, A. Aspect, L. Sanchez-Palencia, D. Delande, B. Grémaud, C.A. Müller and C. Miniatura, "One-dimensional Anderson localization in certain correlated random potentials", Phys. Rev. A **80**, 023605 (2009).
[22] J.P. Dalhaus, J.M. Edge et al, Phys. Rev. B **84**, 115133 (2011)
[23] C. Tian et al, Phys. Rev. Lett. **107**, 074101 (2011).
[24] H. Wang et al., arXiv:1306.6128.
[25] B. Gadway et al., Phys. Rev. Lett. **110**, 190401 (2013).
[26] J. Chabé, H. Lignier, H.L.D. de Souza Cavalcante, D. Delande, P. Szriftgiser and J.C. Garreau, Phys. Rev. Lett. **97**, 264101 (2006): "Quantum scaling laws in the onset of dynamical delocalization"
[27] In this section, we take the kicking period T as unit of time.
[28] Measuring the average $< p^2(t) >$ is tedious and very sensitive to noise in the wings of the momentum distribution. It is much easier to measure the atomic population $\Pi_0(t)$ at zero momentum. Because of atom number conservation, $< p^2(t) >$ is roughly proportional to $1/\Pi_0^2(t)$. The proportionality factor depends on the shape of the distribution, but does not show large changes. As we are interested in scaling properties, $1/\Pi_0^2(t)$ or $< p^2(t) >$ are essentially equivalent.
[29] This also occurs for 1d Anderson localization in a speckle potential [20]: Because the localization length and time vary rapidly with energy, one observes localization at low energy and apparently diffusive behavior at high energy. In between, an apparent mobility edge appears [21], which should not be confounded with the true Anderson metal-insulator transition taking place in the thermodynamic limit, although the experimental signatures may be similar.
[30] The localization length may also depend on ω_2 and ω_3. The mapping on a 3d Anderson model shows that these parameters just affect the *realization* of the disorder, not its statisical properties. Thus, the localization length should not depend on them. This is what is experimentally observed, see section III E.